XLVI CILAMCE
VITÓRIA - ES - BRAZIL - 2025
XLVI IBERO-LATIN AMERICAN CONGRESS ON COMPUTATIONAL METHODS IN ENGENEERING

Strategies to Enhance Column Robustness and Reduce CO_2 Emissions in Progressive Collapse Scenarios: A Risk-Based Optimization Approach

Luiz Eduardo Gonçalves de Mattos[1], Mariana Borges Oliveira[2], André Teófilo Beck[1]

[1]*Dept. of Structural Engineering, University of São Paulo*
[2]*Institute of Architecture and Urbanism, University of São Paulo*
Av Trabalhador São-carlense, 400, 13566-590, São Carlos, SP, Brazil
luizmattos@usp.br, mborgesoliveira@usp.br, atbeck@sc.usp.br

Abstract. Designing robust structures against low-probability, high-consequence events such as fires and vehicular impacts is a critical engineering challenge. These events can trigger progressive collapse, and while traditional strengthening methods can mitigate this risk, they often incur high economic and environmental costs. In this context, this paper employs a Risk-Based Optimization (RBO) framework to identify safer, cost-effective, and more sustainable solutions for a flat-slab parking garage. The study performs a direct comparison between columns designed with conventional Normal Strength Concrete (NSC) and those using Ultra-High Performance Fiber-Reinforced Concrete (UHPFRC). The results reveal the compelling conclusion that the UHPFRC design optimized for cost is not only the most reliable but also presents a lower total expected cost and environmental impact than its NSC counterparts. This demonstrates that advanced materials, when evaluated through a holistic risk-based lens, can provide solutions that are simultaneously safer, more economical, and more sustainable.

Keywords: risk-based optimization, reliability analysis, progressive collapse, UHPFRC, multi-hazard.

1 Introduction

Designing structural systems to withstand low-probability, high-consequence events is a key challenge in structural engineering [1]. Central to this challenge is the concept of structural robustness: a system's ability to prevent localized damage from escalating into disproportionate consequences, such as progressive collapse.

The inherent risks of progressive collapse have spurred extensive research into new design guidelines, preventive methodologies, and mitigation measures [2, 3].

Kiakojouri et al. [4] classify progressive collapse mitigation techniques into three stages: preventing initial damage, controlling propagation, and limiting the final collapse size. The Alternate Load Path (ALP) method is a prominent strategy that primarily addresses the second stage by enhancing structural redundancy, typically through the strengthening of core elements (e.g., by increasing cross-sections).

Despite its effectiveness, implementing the ALP method via conventional strengthening faces significant hurdles. It can be constrained by economic factors [4] and, moreover, often entails a high environmental cost, as increasing material consumption directly raises the structure's embodied greenhouse gas emissions.

Ultra-High Performance Fiber-Reinforced Concrete (UHPFRC) is an innovative material investigated due to its superior mechanical properties, including high strength, ductility, and impact resistance [5]. However, the high cement consumption required for its production raises significant economic and environmental concerns, potentially rendering the material unviable.

To address these competing demands, this paper applies a Risk-Based Optimization (RBO) framework to the design of a flat-slab parking garage, assessing its vulnerability to progressive collapse under multi-hazard scenarios (fire and vehicular impact in columns). This approach provides a rational basis for design by balancing structural safety against progressive collapse with both economic and environmental costs. Specifically, this study evaluates and compares two distinct design approaches for the building's columns: one employing conventional Normal Strength Concrete (NSC, f_{ck} = 30 MPa) and another using a modern UHPFRC (f_{ck} = 120 MPa). By optimizing each material choice as a separate problem, this work identifies the most efficient structural solutions considering both cost and sustainability.

2 Structural Model and Analysis Methods

This study investigates reinforced concrete flat-slab parking garages under two distinct hazards: fire and vehicular collision in columns. Such structures are susceptible to progressive collapse initiated by punching shear failure, particularly following a column loss. The fire risk in these occupancies may be exacerbated by the increasing prevalence of electric vehicles and the potential integration of refueling or charging stations.

The reference structure is a ten-story building with a total height of 30 m (3 m per story). It features a symmetrical column layout with a 4x4 grid on each floor, resulting in 16 columns per story. The span between columns is 8 m in both orthogonal directions, as illustrated in Fig. 1.

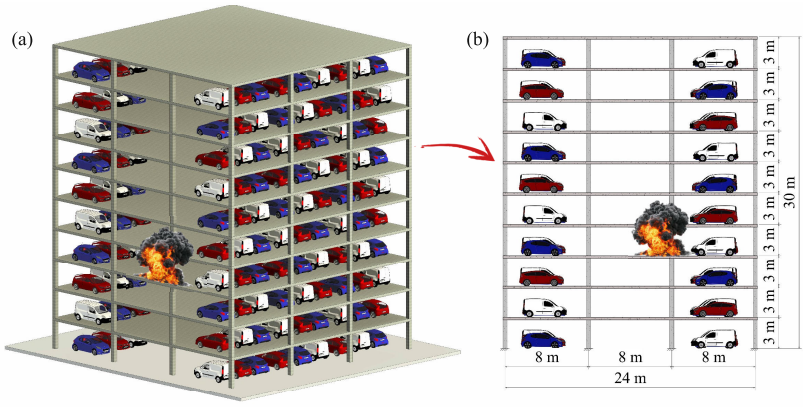


Figure 1. Structural model and analysis approach: (a) 3D view of the reference parking garage and (b) 2D equivalent frame simplification implemented for the FEM analysis.

The column dimensions are the design variables of the optimization problems; therefore, they depend on the resulting optimal solution. All columns within the building share the same cross-section and material. They are composed of either Normal Strength Concrete (NSC, $f_{ck} = 30$ MPa) or Ultra-High Performance Fiber-Reinforced Concrete (UHPFRC, $f_{ck} = 120$ MPa), and are reinforced with four longitudinal steel bars ($f_{yk} = 500$ MPa). For both concrete types, a minimum reinforcement ratio of 0.8% of the gross cross-sectional area is adopted [6]. Transverse reinforcement is provided by 6.3 mm diameter stirrups spaced at 150 mm.

The flat slabs, composed of NSC, have a uniform thickness of 25 cm on all floors. In contrast to the columns, the slab design is kept constant and is not included as a variable in the optimization problem. The flexural reinforcement and punching shear capacity were determined in accordance with ABNT NBR 6118:2023 [6]. This verification indicated that no shear reinforcement was required, and a longitudinal reinforcement of 5 cm^2 per meter of slab width is provided in all spans.

The structural analysis was performed using the Finite Element Method (FEM). Numerical models were implemented in the open-source software OpenSees [7], employing linear beam elements and principles of the Equivalent Frame Method (EFM). The EFM is a technique that simplifies the 3D slab system into a series of 2D frames [8], as shown in Fig.1(b).

2.1 Failure Criteria and Limit States

The structural analysis encompasses three distinct scenarios: normal load conditions, fire exposure, and vehicular impact. In the two exceptional scenarios (fire and impact), columns are identified as the critical structural elements due to their direct exposure to these hazards. The failure criteria for each scenario are detailed below.

The analysis of columns under fire exposure consists of two main stages. First, a thermal analysis simulates a 120-minute exposure to the standard hydrocarbon "H" fire curve, which represents severe fire conditions typical of parking garages. Heat transfer within the column cross-section is solved using the Finite Difference Method. This analysis incorporates the temperature-dependent thermal properties of NSC and UHPFRC, with data sourced from Eurocode [9] and Bolina et al. [10], respectively. Second, a structural analysis using the Deformation Compatibility Method (DCM) determines the column's load-bearing capacity at elevated temperatures [11]. This iterative method yields the moment-curvature relationship, generalized stiffness, and the axial force-bending moment (N-M) interaction diagram, accounting for the degradation of the concrete and steel constitutive laws with temperature. Finally, the failure criterion is defined by a limit state equation based on the minimum load path, which establishes a linear relationship between axial force and bending moment for a constant eccentricity.

For the vehicular impact scenario, shear failure is considered the governing failure mode, as highlighted by Abdelkarim and ElGawady [12]. The column's shear capacity is calculated differently for each material. For NSC columns, the formulation from ACI 318:2019 [13] is adopted, while for UHPFRC columns, the method from the French standard [14] is used. Both models account for contributions from the concrete and transverse reinforcement; the UHPFRC model additionally includes the contribution from steel fibers. The shear demand is derived from the impact, calculated as an equivalent static force using a quasi-static model [12]. This model converts the vehicle's mass, stiffness, and impact velocity into a load applied at a height of 1 meter on the target column.

Under normal load conditions, the column's failure is defined by its N-M interaction diagram. This diagram is generated using the same DCM methodology, but with material properties defined at room temperature (20 °C) and omitting the preliminary thermal analysis.

The system's resistance to progressive collapse is evaluated using the ALP method, which assesses the structure's capacity to redistribute loads after element removal. The analysis simulates the removal of corner and central columns on each story, as well as the sequential loss of two adjacent columns. The failure criterion for the remaining elements depends on the initiating hazard: in a fire scenario, the capacity of adjacent columns accounts for temperature-induced material degradation, whereas in an impact scenario, they are assessed under redistributed loads at room temperature.

3 Structural reliability analysis

This study employs the First-Order Reliability Method (FORM) to calculate the reliability index, β. The corresponding failure probability (p_f) is then given by $p_f = \Phi(-\beta)$. The random variables considered in this analysis are presented in Table 1.

Table 1. Random variables affecting building performance

Variable	Nominal value	Mean	SD	Distribution	Ref.
Dead load (D)	6.25 kN/m²	$1.05D_n$	$0.105D_n$	Normal	[15]
Live load in normal condition (L_{NLC})	2.5 kN/m²	L_n	$0.25L_n$	Gumbel	[15]
Live load in hazard condition (L_H)	2.5 kN/m²	$0.245L_n$	$0.147L_n$	Gumbel	[11]
Fire temperature (θ)	"H" curve [9] °C	θ_n	$0{,}45\theta_n$	Normal	[16]
Vehicle mass (m)	2131 kg	m_n	$0.33m_n$	Normal	[17]
Vehicle speed (v)	40 km/h	v_n	$0.15v_n$	Log-normal	[17]

While material strengths (f_{ck} and f_{yk}) are inherently uncertain, a preliminary sensitivity analysis indicated that their variability has a minimal impact on the reliability results. Therefore, to reduce the computational cost, these parameters are treated as deterministic, using their respective mean values.

A progressive collapse scenario is modeled as a sequence of failures initiated by a given hazard, H, which has an annual probability of occurrence p_H. The sequence begins with the initial **Column Loss (CL)**, defined as the failure of a column due to the hazard. Its total probability of occurrence is given by $p_{CL} = \sum_H P[CL|H]p_H$. This event is followed by **Slab Loss (SL)**, which represents the failure of the slab system as a consequence of the column loss, with a total probability of $p_{SL} = \sum_H \sum_{CL} P[SL|CL, H]P[CL|H]p_H$. The sequence culminates in **Global Collapse (GC)**, characterized by the cascading failure of subsequent floors. The global collapse probability is given by $p_{GC} = \sum_H \sum_{CL} \sum_{SL} P[GC|SL, CL, H]P[SL|CL, H]P[CL|H]p_H$ [11].

Following the framework proposed by Beck and Stewart [1], the analysis integrates both normal and accidental scenarios. This is achieved by treating the normal load condition (NLC) as a "hazard" with a probability of occurrence of unity ($p_{NLC} = 1$). The other two hazards considered are fire and vehicular impact. Their annual probabilities of occurrence, p_{fire} and p_{impact}, are varied across the range $[10^{-5}, 10^{-4}, 10^{-3}, 10^{-2}, 10^{-1}]$. This combination results in the set of hazard scenarios considered in the analysis.

Previous studies on flat-slab structures have shown that the conditional probability of slab failure following a single column loss, $P[SL|CL, H]$, is close to one, highlighting the system's vulnerability [8, 11]. However, to account for three-dimensional load redistribution effects not explicitly captured by the 2D frame model, a different assumption is adopted in this work. It is considered that the slab system can withstand the loss of a single column ($P[SL|C_1L, H] = 0$) but will collapse upon the sequential loss of a second adjacent column ($P[SL|C_2L, C_1L, H] = 1$).

4 Risk-based Optimization

Risk is formally defined as the product of an event's probability of occurrence and the magnitude of its consequences, which are often measured in terms of cost [1]. Since any structure has a non-zero, although small, probability of failure, accounting for the expected failure costs is essential. Risk-Based Optimization (RBO) is a framework designed to balance safe and economically efficient solutions for structural systems by minimizing a total expected cost function.

The total expected cost (C_{TE}) represents the sum of all costs incurred throughout a structure's lifecycle. The RBO problem is thus formulated as finding the optimal design variables for both NSC and UHPFRC columns, $\mathbf{d}^{NSC^*} = \left\{h^{NSC^*}, b^{NSC^*}\right\}$ and $\mathbf{d}^{UHPFRC^*} = \left\{h^{UHPFRC^*}, b^{UHPFRC^*}\right\}$, which minimize:

$$C_{TE}(\mathbf{X}, \mathbf{d}) = C_M(\mathbf{d}) + C_{CL}(\mathbf{d})p_{CL}(\mathbf{X}, \mathbf{d}) + C_{GC}(\mathbf{d})p_{GC}(\mathbf{X}, \mathbf{d}), \tag{1a}$$

subject to

$$\begin{gathered} 30 \leq h^{NSC} \leq 60\ ,\ 30 \leq b^{NSC} \leq h^{NSC}\ ,\ \text{and} \\ 20 \leq h^{UHPFRC} \leq 40\ ,\ 20 \leq b^{UHPFRC} \leq h^{UHPFRC}, \end{gathered} \tag{1b}$$

where h and b are the cross-section dimensions (in cm), with the analysis considering bending about the axis of greatest inertia (i.e., the axis parallel to the dimension b); and $\mathbf{X}$ is the random variable vector.

C_{TE}, evaluated independently for C_{TE}^{NSC} and C_{TE}^{UHPFRC} designs, comprises the following three terms:

1. C_M, the initial construction cost, encompassing materials (concrete, reinforcement), formwork, and labor. Cost data were sourced from the Brazilian SINAPI database [18], reflecting prices for São Paulo (April 2025), with values converted from BRL to USD (1 USD = 5.5 BRL). The resulting unit cost for ready-mix NSC (C30) is 91.20 USD/m^3. Due to the lack of standardized pricing for UHPFRC, its cost was estimated at approximately 400 USD/m^3 based on its constituent materials. Costs for reinforcement and formwork are included in the total but not detailed here for brevity;
2. The expected cost of global collapse, defined as a multiple of the initial cost ($C_{GC} = 80 \times C_M$), multiplied by the global collapse probability (p_{GC});
3. The expected cost of local damage, defined as a fraction of the initial cost ($C_{CL} = 0.2 \times C_M$), multiplied by the column loss probability (p_{CL}).

The cost factors for C_{GC} and C_{CL} are based on the severe consequences of failure in a ten-story parking garage. These include potential loss of life and assets, panic situations, and fire propagation.

This work extends the RBO framework to an environmental perspective by using the Global Warming Potential (GWP) as the consequence metric. GWP measures greenhouse gas emissions in kilograms of CO_2 equivalent ($kgCO_2eq$) and is a key indicator in structural life cycle assessments [19]. The objective is to minimize embodied emissions in a "cradle-to-gate" assessment by finding the optimal design variables $\mathbf{d}^*$ that minimize the total expected GWP:

$$GWP(\mathbf{X}, \mathbf{d}) = CO_{2,M}(\mathbf{d}) + CO_{2,GC}(\mathbf{d})p_{GC}(\mathbf{X}, \mathbf{d}), \tag{2}$$

subject to the same Eq. (1b) bounds constraints.

Similarly, GWP, evaluated independently for the two materials designs, comprises the following two terms:

1. $CO_{2,M}$, the embodied emissions from the manufacturing phase ("cradle-to-gate"). This includes emissions from material production (concrete, steel) and transport to the construction site (assumed 20 km). Based on the SIDAC database [19], the emission factors are 283.8 $kgCO_2eq/m^3$ for ready-mix NSC and 536.69 $kgCO_2eq/m^3$ for UHPFRC [20];
2. The expected emissions from global collapse ($CO_{2,GC} = 1.25 \times CO_{2,M}$), multiplied by its probability (p_{GC}). This term encompasses emissions from demolition, reconstruction, and related activities.

It should be noted that the GWP associated with local damage (column loss) is not included in this formulation. While such an event carries an environmental impact, preliminary analyses indicated its contribution is negligible compared to the manufacturing and global collapse terms.

5 Results

This study performs four distinct RBO analyses by combining two objective functions, total expected cost, Eq.(1a), and total expected GWP, Eq.(2), with two column materials (NSC and UHPFRC). Each of these four analyses was solved for 25 different hazard scenarios, resulting in a total of 100 optimization runs.

A key finding of this study is that the optimal column dimensions (h and b) are highly sensitive to the annual probability of the initiating hazard (p_H), with this effect being especially pronounced for UHPFRC columns. Figure 2 illustrates this trend, presenting the optimal designs for both (a) NSC and (b) UHPFRC columns under each optimization objective. As the perceived risk (i.e., a higher p_H) increases, the optimization consistently demands more robust column sections.

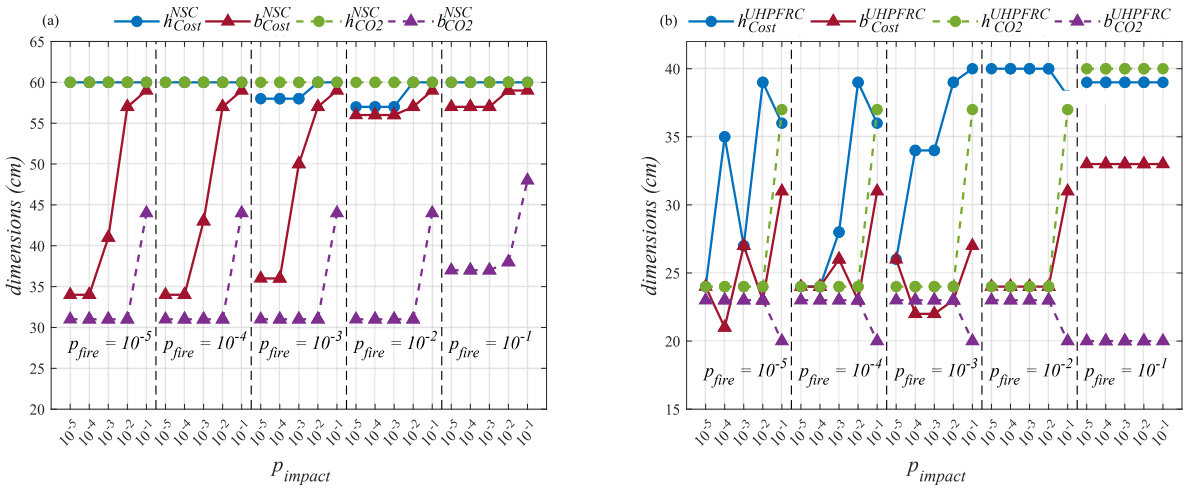


Figure 2. Optimal column dimensions for (a) NSC and (b) UHPFRC designs from cost and CO_2 minimization across different hazard probabilities.

Analysis of the results reveals observations. First, cost-based optimization consistently yields more robust column designs (i.e., larger cross-sections) than GWP-based optimization for both NSC and UHPFRC. Second, the optimal designs frequently favor taller, more slender sections, with the column height (h) often approaching its upper bound constraint. This geometric preference maximizes the moment of inertia for a given area, thereby enhancing the capacity to resist combined axial force and bending moment (N-M).

This trend is especially pronounced in high-risk scenarios. For instance, to minimize cost under a high fire probability ($p_{fire} = 10^{-1}$), the optimal NSC column design expands to its maximum allowable dimensions. This outcome demonstrates a critical trade-off: when the probability of a hazard is high, the expected cost of failure ($p_{GC} \times C_{GC}$) dominates the total cost function, forcing the optimization to prioritize structural reliability far above initial material savings.

Figure 3 presents a cross-analysis of the results. Subplot (a) shows the total expected cost and subplot (b) shows the total expected GWP for the optimal designs derived from both the cost-minimization and GWP-minimization frameworks.

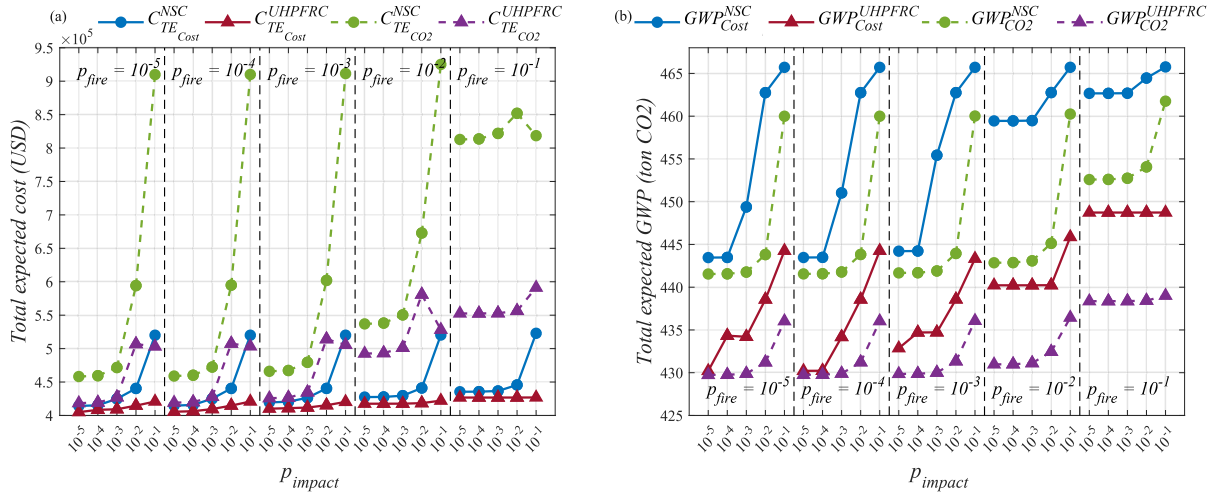


Figure 3. Trade-offs between cost and CO_2 emissions, showing (a) the total expected cost and (b) the total expected GWP for optimal designs across different hazard probabilities.

From an economic perspective, the results reveal a compelling, and potentially counter-intuitive, advantage for UHPFRC. In all evaluated scenarios, UHPFRC designs consistently yield a lower total expected cost (C_{TE}) than their NSC counterparts. Specifically, when both materials are optimized for cost, the optimal NSC solution is 18.3% more expensive than the UHPFRC alternative; this cost disparity widens to a remarkable 44.5% when comparing the GWP-optimized designs. This outcome is driven by UHPFRC's superior performance, which allows for smaller sections and drastically lower failure probabilities. This reduction in the risk-weighted failure cost ($p_{GC} \times C_{GC}$) more than compensates for UHPFRC's higher initial material price.

From an environmental standpoint, UHPFRC's superiority is also evident. The UHPFRC solutions produce a lower GWP than the NSC solutions, even when the NSC design is optimized specifically for environmental performance. This critical insight shows that while UHPFRC has a higher embodied GWP per cubic meter, its efficiency leads to significantly smaller material volumes and lower collapse probabilities. The combined effect results in a net environmental benefit. Although the percentage reduction is more modest than the cost savings—with UHPFRC being approximately 5.2% better in the most favorable scenario—this translates into a significant absolute decrease of nearly 24 tonnes of CO_2eq, a noteworthy contribution for a single building project.

To assess the safety level of the optimal designs, Fig.4 presents the reliability index associated with global collapse (β_{GC}) for each framework.

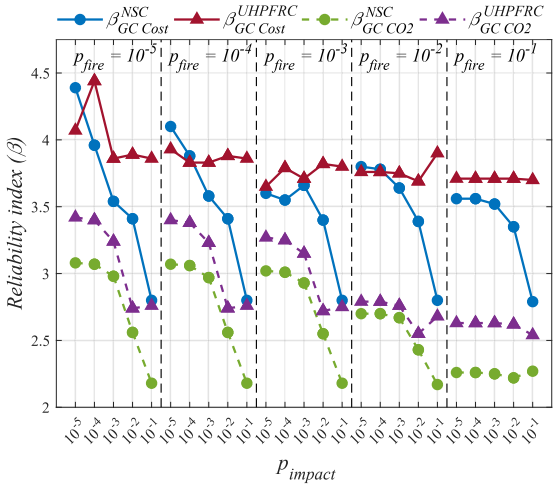


Figure 4. Global collapse reliability index for each optimal design framework across different hazard probabilities.

The cost-optimized UHPFRC solution stands out for its exceptional reliability performance, that consistently maintains $\beta^{UHPFRC}_{GC\ Cost} > 3.5$ across all hazard scenarios, demonstrating remarkable stability even as the perceived risk increases. In contrast, the cost-optimized NSC solution exhibits significant vulnerability under high-risk of vehicular impact. While achieving acceptable reliability in lower-risk scenarios, its safety level drops sharply for high-probability events, with $\beta^{NSC}_{GC\ Cost} < 3$ for the $p_{impact} = 10^{-1}$ case.

The trade-off between sustainability and safety becomes evident when analyzing the GWP-optimized designs. The NSC solution proves inadequate from a reliability standpoint, with $\beta^{NSC}_{GC\ CO2}$ falling below 3 for most scenarios and dropping to as low as 2.2 under high risk. The UHPFRC solution, in contrast, offers a much safer environmental alternative, successfully maintaining $\beta^{UHPFRC}_{GC\ CO2} > 3$ for all low-probability hazard scenarios ($p_H \leq 10^{-3}$).

6 Conclusions

This paper presented a risk-based optimization framework to assess the economic and environmental performance of flat-slab buildings under multi-hazard scenarios (fire and vehicular impact) with columns designed with Normal Strength Concrete (NSC) and Ultra-High Performance Fiber-Reinforced Concrete (UHPFRC).

The most compelling finding is that the cost-optimized UHPFRC design emerged as the superior solution overall. This framework not only yielded the lowest total expected cost but also produced the second-lowest GWP, all while consistently maintaining the highest and most stable reliability index across all hazard scenarios. This demonstrates that investing in a high-performance material can lead to a solution that is simultaneously safer, more economical, and more sustainable when evaluated from a holistic, risk-based perspective.

Furthermore, this study highlights that a single-objective GWP minimization can lead to designs with inadequate reliability under high-risk conditions. This suggests that future research should focus on multi-objective

optimization frameworks and minimum target reliability index constraints. Such an approach would enable the identification of compromise solutions (a Pareto front) that balance economic and environmental goals while satisfying a prescribed minimum level of structural safety.

Acknowledgements. Funding for this research project by CNPq (National Council for Scientific and Technological Development, grant n. 309107/2020-2) and joint FAPESP-ANID (São Paulo State Foundation for Research - Chilean National Agency for Research and Development, grant n. 2019/13080-9) and FAPESP (grant n. 2024/23665-2) is also gratefully acknowledged.

Authorship statement. The authors hereby confirm that they are the sole liable persons responsible for the authorship of this work, and that all material that has been herein included as part of the present paper is either the property (and authorship) of the authors, or has the permission of the owners to be included here.

References

[1] A. T. Beck and M. G. Stewart. Risk-based cost-benefit analysis of structural strengthening to mitigate disproportionate collapse of buildings under abnormal blast loading. *Structures*, vol. 57, pp. 105103, 2023.
[2] U. Starossek. *Progressive collapse of structures*, volume 153. thomas telford London, 2009.
[3] J. M. Adam, F. Parisi, J. Sagaseta, and X. Lu. Research and practice on progressive collapse and robustness of building structures in the 21st century. *Engineering Structures*, vol. 173, pp. 122–149, 2018.
[4] F. Kiakojouri, V. Biagi, B. Chiaia, and M. R. Sheidaii. Progressive collapse of framed building structures: Current knowledge and future prospects. *Engineering Structures*, vol. 206, pp. 110061, 2020.
[5] de A. M. Sousa, E. O. Lantsoght, A. S. Genikomsou, P. A. Krahl, and K. Mounir. Behavior and punching capacity of flat slabs with the rational use of uhpfrc: Nlfea and analytical predictions. *Engineering Structures*, vol. 244, pp. 112774, 2021.
[6] ABNT. *Associação Brasileira de Normas Técnicas. NBR 6118 - Projeto de Estruturas de Concreto*. Rio de Janeiro, 2023.
[7] F. McKenna. Opensees: a framework for earthquake engineering simulation. *Computing in Science & Engineering*, vol. 13, n. 4, pp. 58–66, 2011.
[8] J. C. C. B. Carneiro, de L. E. G. Mattos, and A. T. Beck. Reliability analysis of the simplified punching shear resistance model of eurocode 2: 2004 in different column positions on flat slabs. In *Ibero-Latin American Congress on Computational Methods in Engineering (CILAMCE)*, 2024.
[9] Eurocode. Design of concrete structures 1-2: General rules-structural fire design (en 1992-1-2), 2004.
[10] F. L. Bolina, G. Poleto, and H. Carvalho. Proposition of parametric data for uhpc at high temperatures. *Journal of Building Engineering*, vol. 76, pp. 107222, 2023.
[11] de L. E. G. Mattos, J. C. C. B. Carneiro, and A. T. Beck. Risk-based optimum design of a device to simultaneously protect building columns against accidental impact, fire and progressive slab collapse. *Engineering Structures*, vol. 332, pp. 119983, 2025.
[12] O. I. Abdelkarim and M. A. ElGawady. Performance of bridge piers under vehicle collision. *Engineering Structures*, vol. 140, pp. 337–352, 2017.
[13] A. Committee. Building code requirements for structural concrete (aci 318-19) and commentary. American Concrete Institute, 2019.
[14] N. P. 18-710. National addition to eurocode 2—design of concrete structures: specific rules for ultra-high performance fibre-reinforced concrete (uhpfrc), 2016.
[15] D. O. Ellingwood. Building design for abnormal loads and progressive collapse. *Computer-Aided Civil and Infrastructure Engineering*, vol. 20, n. 3, pp. 194–205, 2005.
[16] C. D. Eamon and E. Jensen. Reliability analysis of reinforced concrete columns exposed to fire. *Fire safety journal*, vol. 62, pp. 221–229, 2013.
[17] R. Thomas, K. Steel, and A. D. Sorensen. Reliability analysis of circular reinforced concrete columns subject to sequential vehicular impact and blast loading. *Engineering Structures*, vol. 168, pp. 838–851, 2018.
[18] SINAPI. Sistema nacional de pesquisa de custos e índices da construção civil. referência de preços e custos (in portuguese). Accessed: 7 June 2025, 2025.
[19] F. B. Silva, L. S. Oliveira, D. d. C. Reis, G. T. G. Pato, A. C. Marinho, C. M. Degani, L. R. Caldas, K. R. G. Punhagui, S. A. Pacca, and V. M. John. The sidac system: streamlining the assessment of the embodied energy and co2 of brazilian construction products. *Journal of Cleaner Production*, pp. 01–35, 2023.
[20] L. Bouhaya, R. Le Roy, and A. Feraille-Fresnet. Simplified environmental study on innovative bridge structure. *Environmental science & technology*, vol. 43, n. 6, pp. 2066–2071, 2009.